Molecularly Imprinted Polymer Modified Glassy Carbon Electrodes for the Electrochemical Analysis of Isoproturon in Water

Imer Sadriu[a,b] , Sarra Bouden[a], Jimmy Nicolle[a], Fetah I. Podvorica[b] , Valérie Bertagna[a], Catherine Berho[c], Laurence Amalric[c] and Christine Vautrin-Ul[a*]

[a] *ICMN Interfaces, Confinement, Matériaux et Nanostructures, UMR7374 - Université d'Orléans–CNRS, 1b rue de la Férollerie, 45071 Orléans Cedex 2, France*

[b] *Chemistry Department of Natural Sciences Faculty, University of Prishtina, rr. "Nëna Tereze" nr. 5, 10000 Prishtina, Kosovo*

[c] *BRGM, Bureau de Recherches Géologiques et Minières, Laboratory Division, 3 avenue Claude Guillemin, 45060 Orléans Cedex 2, France*

**Corresponding authors: christine.vautrin-ul@cnrs-orleans.fr;*

Abstract:

Isoproturon-imprinted polypyrrole films were electrochemically synthesized onto glassy carbon (GC) electrodes in an ethanol/aqueous solution of pyrrole as a monomer, isoproturon as a template molecule and $LiClO_4$ as supporting electrolyte. Electropolymerization was performed by cyclic voltammetry and chronoamperometry. The isoproturon template molecules were successfully trapped in the polypyrrole film where they created artificial recognition cavities. After the electrochemical extraction of the template, the polypyrrole film acted as a molecularly imprinted polymer (MIP) for the selective recognition of isoproturon whereas the non-imprinted polymer (NIP) film, made in the same conditions except for the presence of isoproturon, did not exhibit any interaction. The MIP and NIP films were characterized by cyclic voltammetry in the presence of redox probes and the thickness of the polymer layers was estimated by EQCM (Electrochemical Quartz Crystal Microbalance) and calculated using Faraday's law. The isoproturon-imprinted polypyrrole films were found to selectively detect isoproturon even in the presence of the interferents carbendazim and carbamazepine. Its limit of detection (LOD) in milli Q water, achieved via square wave voltammetry was as low as 0.5 µg L^{-1}, whereas in real water samples it was found to be 2.2 µg L^{-1}.

Keywords: Electrochemical sensors, polypyrrole films, molecularly imprinted polymers, isoproturon detection.

1 Introduction

The use of many herbicides in agriculture, although beneficial for food production and prevention against nuisance organisms, can lead to their release into the environment where they have a negative impact on the ecosystem and human health. Furthermore their degradation products and metabolites are toxic toward living organisms. Systematic quality monitoring of groundwater and surface water showed that many aquifers have been contaminated by these pollutants. Isoproturon (3-(4-isopropylphenyl)-1,1-dimethylurea or 3-p-cumenyl-1,1-dimethylurea), a herbicide belonging to the phenyl urea family, is widely used to kill weeds in soils [1

]. Recent studies indicated that isoproturon has become an ecosystem contaminant due to its intensive use [2] and in 2016, the EU decided to ban its use. Isoproturon has been detected worldwide in soil, groundwater, surface water, or even in drinking water, exceeding the threshold values (e.g., the European Union threshold is 0.1 μg L^{-1}). Raw waters may become contaminated with isoproturon from production plant discharges and diffuse agricultural sources [3].

According to the World Health Organization (WHO), isoproturon has demonstrated toxicity to the liver system and appears to be a tumor promoter [4]. Considering its hazardous effects, the European Union (EU) has classified it as a priority micro-pollutant and has regulated its maximum levels at 0.3 μg L^{-1} for inland surface waters [5]. It is therefore necessary to develop sensitive and selective techniques to monitor its presence in natural aquatic environments. Sophisticated analytical techniques based on chromatography are frequently used for isoproturon detection in environmental samples [3,6-10] with detection limits between 10 and 100 ng L^{-1} reported [3,5]. However, these techniques, in spite of their high sensitivities, remain expensive and difficult to implement for on-site and *in-situ* analysis. In addition, on-site sampling and its treatment involves a longer analysis time and complex additional steps to overcome matrix effects and interferences [3,5,7]. There is an increasing need to ensure efficient and continuous on-site and *in-situ* monitoring of environmental waters, and to reduce the cost of analysis, which implies developing novel sensors.

Efforts are thus ongoing to develop rapid and inexpensive sensing devices for the detection of pesticides in general and particularly isoproturon. Among all the conventional techniques, electrochemical analysis is one of the simplest and least expensive. Voltammetric-based methods have been widely reported for the determination of many pesticides and isoproturon more specifically using various carbon electrode materials such as glassy carbon [11,12], graphene [13], wall-jet glassy carbon electrode [14], carbon paste [15,16], carbon fiber [17], doped diamond [18], and multiwalled carbon nanotubes (MWCNT) [19]. More recently, numerous studies have focused on modified electrodes [20] and various assemblies have been investigated for applications in isoproturon electrochemical sensors such as clay-modified GC electrodes [21,22], or enzyme-modified [19,23-25] and conducting polymer modified electrodes [26]. The attachment of the organic film on the electrode surface makes it possible to increase the sensitivity and the selectivity of these modified electrodes toward a targeted analyte. Still, one of the most ingenious methods to achieve this goal is to prepare molecularly imprinted polymers [27-30].

A molecularly imprinted polymer (MIP) is obtained by polymerization of a monomer in the presence of a template molecule and a cross-linker agent. After polymerization, the template molecules, trapped in the polymeric matrix, are removed leaving behind cavities that are complementary not just in shape but also in functionalities. The cavities contain functional groups of the polymer that were left in a ‘‘frozen’’ conformation/orientation that leads to the specific uptake of the targeted analyte. High affinity and selectivity are based on the shape of the print together with the specific interactions between the functional groups from the MIPs and the target micro-pollutant [31,32,33].

For sensing issues, the selective recognition of the analyte by the MIPs can be achieved through concentration of the samples via: i) MIP Solid Phase Extraction (SPE) cartridges or membranes [34,35,36] or ii) coated electrodes by *ex-situ* prepared MIP or MIP films deposited *in-situ* at the electrode [37,38,39]. After this concentration step, the analysis can be achieved by several techniques (electrochemical, chromatographic, optical, etc.).

MIPs of different compositions and for different purposes can be prepared in several ways: photo-polymerization [40,41], free radical [42][and controlled radical polymerization [43,44], polymerization by evanescent waves [45][and *in-situ* electropolymerization. For the MIPs used in electrochemical sensing, those prepared by the latter method are more numerous because it is simple, fast and inexpensive. Moreover, electropolymerization allows a better thickness control and adhesion of the polymer layer on the surface of substrates and shows the

ability to attach selective films of any shape and size compatible with commercial and industrial implementation [46]. Various types of electro-synthesized polymers based on molecular imprinting have been reported including polyphenol, polymethacrylic-acid, [47] polyaniline [48,49,50] and polypyrrole [51,52,53,54]. Recently the use of some Metal Organic Frameworks (MOFs) based on the electropolymerization of monomer-functionalized gold nano-particles was reported [55].

Among the abovementioned polymers, polypyrrole films are most advantageous for environmental applications thanks to their easy *in-situ* electropolymerization at the electrode surface with or without the presence of the template molecule [55]. Moreover, the formation of the polypyrrole film is fast and it is well known to be a partially cross-linked polymer so that there is no need to add a cross-linker agent [55]. Extraction and rebinding of the template can be conducted electrochemically since polypyrrole is a conducting polymer, to some extent [55]. In addition, the electropolymerization of polypyrrole leads to chemically and mechanically robust films [56,57].

Therefore, thanks to all these properties, MIPs have inspired researchers in analytical chemistry to address the massive demand for monitoring molecules of interest in different fields such as biology [58,59,60,61], the environment [56,62], food science and technologies [63,64], pharmaceuticals and controlled drug release [65,66].

While the number of studies on the use of MIP-based sensors in pesticide analysis is increasing [67,68,69,70,71], only a few have focused on isoproturon detection, which has been classified as a priority pollutant by the WFD [4].

Li *et al.* [71] developed a new molecularly imprinted polyaminophenol electrochemical luminescence sensor (MIP-ECL sensor) for isoproturon determination based on the competition reaction between isoproturon and glucose oxidase [72]. However, even though the method has provided very low detection limits (0.8 ng L^{-1}), the use of additional reagents, the equipment required and the complex preparation of the samples remain incompatible with *in-situ* measurements.

Singh et al. (2013) developed an *ex-situ* polymethacrylic imprinted polymer solid phase extraction for isoproturon detection [73] and reached a detection limit of 0.2 mg L^{-1} which is unfortunately too high in light of current standards [4]. In addition, an *ex-situ* MIP synthesis involves additional steps, which complicates the implementation of the sensor.

In this context, the aim of the present work was to develop an electrochemically polypyrrole MIP based electrode for the sensitive and selective detection of isoproturon. The influence of the experimental parameters on the characteristics of the polymer matrix and its ability to recognize and to concentrate isoproturon were studied. In order to maximize isoproturon signal detection we adjusted several parameters during the MIP electrosynthesis. The analytical performances of the modified electrodes were then assessed.

2 Experimental

2.1 Reagents and apparatus

Pyrrole, lithium perchlorate, $LiClO_4$, isoproturon (ISO), tetrabutylammonium tetrafluoroborate, acetonitrile, ferrocene, NBu_4BF_4, ethanol, carbamazepine (Cbd), diuron, carbendazim (Cbmz) and sulfuric acid were purchased from Sigma-Aldrich. Electrochemical measurements were carried out using a potentiostat/galvanostat PGSTAT 204 and PGSTAT 128N Autolab Metrohm interfaced with a PC under Nova 2.2 software and three electrodes in a one-compartment cell. The working electrode was a glassy carbon (GC) disc (area of 0.07 cm^2). Ag/AgCl saturated with KCl was used as a reference electrode and a curved platinum wire was used as a counter electrode. The working electrodes were polished before each experiment by using decreasing sizes of diamond paste, rinsed and sonicated with milli-Q water, dried and stored in a clean place. The EQCM measurements were performed with a Maxtek RQCM micro-balance on Maxtek 5 MHz Au-Cr crystals.

2.2 Synthesis of NIP-GC and MIP-GC electrodes

The electro-synthesis of molecularly imprinted polymer (MIP) films and that of non-imprinted polymer (NIP) films was performed on glassy carbon electrodes, respectively named MIP-GC and NIP-GC, in an ethanol and water (20/80) solution containing 10 mM of pyrrole and 0.1 M of $LiClO_4$ as electrolyte. For the preparation of MIP-GC, the template molecule, 1 mM of isoproturon, was added. Electropolymerization was accomplished either by applying cyclic voltammetry (CV), 5 scans in the potential range from 0 to 1.4 V vs Ag/AgCl at a scan rate: v = 10 mV s^{-1}, or by chronoamperometry (CA), with a potential set at 1.1 V vs Ag/AgCl for a duration of 600 s.

The MIP-GC electrodes, once prepared, were rinsed with milli-Q water and immersed in an ethanol/water (70:30 v/v) solution of 0.1 M sulfuric acid. They were biased to a potential excursion between -0.4 V and 1.5 V vs Ag/AgCl for several scans until complete extraction of

the embedded isoproturon molecules. After extraction the MIP-GC electrode was used for isoproturon detection.

2.3 Detection of isoproturon by MIP-GC electrodes

The MIP free of isoproturon and NIP coated electrodes were immersed in an aqueous solution containing isoproturon as template molecule, under stirring, during an optimized time. Both electrodes were then rinsed with milli-Q water in order to remove the isoproturon just deposited on the MIP-GC and NIP-GC surface. The electrochemical detection of isoproturon was achieved by square wave voltammetry (SWV), in an ethanol/water (70:30 v/v) solution containing 0.1 M of sulfuric acid. The preparation of the MIP-GC and the detection steps are presented on Scheme 1.

3 Results and discussion

The electropolymerization of pyrrole in the presence of isoproturon leads to the inclusion of the template molecule in the polymer matrix during polymer growth. Isoproturon extraction by CV creates cavities within the MIP, which are complementary in shape and functionalities to the template molecule. These prints should therefore allow selective rebinding by isoproturon, as the artificial receptors are shaped by the template [55], and finally the use of SWV will enable to confirm the presence and to determine isoproturon concentration.

3.1 Electropolymerization of pyrrole

As mentioned in section 2.2, the electrochemical polymerization of pyrrole on the GC electrode surface was performed by cyclic voltammetry with and without the presence of the template isoproturon in the monomer solution, see Figure 1.

In both cases, we can observe the anodic current that increase after 0.75 V vs Ag/AgCl due to the oxidation of the pyrrole on GC electrode with the current peak at 0.95 and 1.15 V vs Ag/AgCl respectively in the solutions without and with 1 mM of the ISO template. The potential shift is probably due to the presence of isoproturon in the solution which itself is oxidized at a potential around 1.0 V, see below, Figure S1.

In the second scan, voltammograms of MIP and NIP electropolymerization show that the pyrrole oxidation peak decreases drastically due to the change in the nature of the electrode surface after the deposition of a polypyrrole layer that is less conductive than the carbon itself [74].

3.2 Extraction of the template molecule

The template extraction was achieved by the procedure described in section 2.2 by cyclic voltammetry (voltammograms in Supplementary Material Figure S1). We observed an oxidation peak, at around 1 V vs Ag/AgCl, corresponding to the isoproturon trapped within the polymeric matrix.

Several scans were made until the oxidation peak was no longer observed due to the release of the isoproturon.

The well-known reversible oxidation-reduction behavior of polypyrrole [75] is also clearly observed at 0.4 V vs Ag/AgCl for the polypyrrole oxidation process and -0.25 V vs Ag/AgCl for the reduction process in our MIP-GC electrode.

On the voltammogram of the NIP electrode (not shown), no peak at 1.0 V was observed while the polypyrrole signal was present in the same region as for the MIP.

This method of template extraction is easy to achieve and avoids the use of a variety of chemical reagents. Moreover, the voltammograms obtained validated the removal of the template.

3.3 Optimization of the eletropolymerization procedure for the MIP-GC electrode

In this section, the detection signal of isoproturon served as a tool for the electrochemical synthesis optimization of the MIP-GC electrode. The ISO detection was performed as follows: after the electrochemical release of ISO, MIP-GC electrodes were immersed in a 5 x 10^{-7} M isoproturon water solution during 15 minutes and the analyses were performed by SWV in an ethanol/water solution (70:30 v/v) of 0.1 M sulfuric acid.

The sensing properties of MIP-GC electrodes obtained by CV and by CA were compared after optimizing the impact of the scan number for CV and the electrolysis time for CA and establishing the influence of the ratio of ethanol in the electrolyte solution.

3.3.1 Preparation of isoproturon MIP-GC electrodes by cyclic voltammetry (CV): influence of the scan number

In order to determine the effect of the number of cycles during electropolymerization on the response of isoproturon detection by MIP-GC, the film was prepared with 1, 3 and 5 cycles, see Figure 2A.

It clearly shows that the response of isoproturon is improved with the number of scans due to the increase in the thickness of the polymeric matrix and consequently the number of cavities.

In order to verify this assumption, the theoretical thickness of the layer was estimated from the electrical charge (Figure 2B). To correlate polypyrrole thickness x (cm) and electrical charge, Faraday's law was used assuming 100% current efficiency for polypyrrole:

$$x = qM/\rho AzF$$

where q (C) is the electrical charge associated with polypyrrole formation, M (g/mol) is the molar mass of the monomer, F is Faraday's constant (C mol^{-1}), A (cm^2) is the area of the working surface, ρ (g cm^{-3}) is the polymer density and z (mol) is the number of electrons involved in the electropolymerization process of pyrrole which in this case is 2.25 [76,77]. The nominal density for polypyrrole films (ρ) was taken as 1.5 g cm^{-3} [75]. By taking into consideration all the above-mentioned parameters, the required charge density to grow a film with an average thickness of 290 nm is 10.4 mC.cm^{-2} [76]. We can see, in Fig. 3B, that the estimated thickness increases with the number of cycles to reach 290 nm after 5 scans in the case of MIP-GC.

To confirm this result, the behavior of a ferrocene 2.5 mM redox probe in acetonitrile solution containing 0.1 M NBu_4BF_4 on MIP layers obtained at 1, 3 and 5 cycles was studied (Figure 2C). It shows that the blocking effect for the ferrocene signal increases with the number of cycles due to the growth of the insulating polymer layer because of the over-oxidation conditions [73].

Finally, in order to determine the electropolymerization efficiency, one experimental thickness of the MIP layer deposited by EQCM assuming a density of MIP 1.5 g cm^{-3} [74,75] and the corresponding charge was measured. The electropolymerization yield was calculated from the ratio between the experimental and the theoretical thicknesses and was found to be close to 63%.

3.3.2 Preparation of isoproturon MIP-GC electrodes by chronoamperometry (CA):

3.3.2.1 Effect of solvent: the role of the ethanol/water ratio

During the electropolymerization of a MIP film (see section 2.2), knowing that the solubility of isoproturon is limited in water (70.2 mg/L at 25°C) we added ethanol in water at different quantities. Figure 3A shows the film thickness calculated from chronoamperometry curves for a constant electropolymerization time using Faraday's law for different ratios of ethanol. It is shown that the thickness of the MIP film produced is directly dependent on the amount of ethanol, hence when the amount of ethanol is greater than 40% the film thickness is less than

50 nm. Below 40% of ethanol, the film thickness increases linearly until it is six-fold the initial thickness.

The same MIP-GC electrodes were used for ISO detection. Figure 3B shows the ISO peak current as a function of the ethanol ratio. The best results were achieved with MIP-GC electrodes prepared in water-ethanol solutions containing lower amounts of ethanol. The thickest MIP films were produced with a maximum between 15 and 20% of ethanol. This value was therefore chosen for further study.

3.3.2.2 Influence of electropolymerization time

The influence of the electropolymerization time was studied for the MIP films prepared by CA at 1.1 V vs Ag/AgCl at different times that were used later for ISO detection. The theoretical thickness of the growing layer was estimated from the chronoamperograms on Figure 4A and a rapid increase in this thickness up to 100 s was observed. Thereafter, its further growth is slowed down, reaching an almost linear increase after 200 s. This is most probably because of the decrease in the electronic transfer due to the thickness of the layer and to the partially insulating character of the MIP.

The electrochemical detection ability of isoproturon on MIP-GC electrodes prepared by CA at different electropolymerization times is presented in Figure 4B. These results are in agreement with those presented in Figure 3A. During the first 100 s, the ISO detection signal was very significant, corresponding to the film thickness growth. From 100 s to 600 s, the signal of the target analyte increased more slowly. We can assume that the blocking effect of the charge transfer limits the oxidation of isoproturon during detection. Moreover, the thicker the film is, the more difficult it is for isoproturon molecules to access the cavities and to reach the conducting surface. The sharp signal decrease after 600 s is probably due to the film breaking during its growth. This assumption was validated with measures made by EQCM, Figure 4C. The sharp mass decline also started after 600 s. It should be noted that the sharp decrease both in the ISO peak detection and in the MIP layer mass was observed for the thickest MIP films but not always at the same time. This fact is due most probably to mechanical constraints in the thick films.

As for CV MIP preparation, see below, the electropolymerization yield obtained from CA with EQCM measurement was calculated and the corresponding charge was found to be close to 66 %. This value is of the same order as that obtained with CV electropolymerization. For

both methods, the charge loss is consistent with the high potentials applied during the MIP-GC preparation.

These results show that the optimal electropolymerization time for the isoproturon response is 600 s. In addition, the sensitivity and the reproducibility of the MIP-GC (results not shown) are better for films prepared by chronoamperometry, which is consistent with the literature [53].

3.4 *Electrochemical detection of isoproturon by the GC-MIP electrode*

3.4.1 Optimization of incubation time

The incubation time is an important factor in the analytical procedure since it will impact the overall time of the analysis. The influence of the incubation time in the range of 0 – 40 minutes on the isoproturon signal responses was evaluated in aqueous media containing 5 x 10^{-7} M of isoproturon. As illustrated in Figure 5 the isoproturon oxidation peak intensity increases proportionally with the incubation time in the first 15 minutes due to its rebinding to the created cavities. Beyond 15 min, the rebinding kinetic slows down, suggesting the beginning of saturation of the cavities or a more difficult access of isoproturon. An incubation time of 15 min was therefore chosen to obtain the best analytical performances for this study. This parameter impacts the quantification: in the linearity domain, the longer the time, the more the lower limit of quantification (LOQ) diminishes. Moreover, a lower incubation time leads to less accurate values because monitoring the immersion time is less easy and the signal is lower.

3.4.2 Electroanalytical performances

3.4.2.1. Calibration curve and determination of LOD/LOQ

In this sub-section, the optimal conditions to achieve the best sensitivity for isoproturon detection were selected: the MIP-GC film obtained by CA at 1.1 V vs Ag/AgCl during 600 s was used and isoproturon detection by SWV was carried out in an ethanol/water solution (70:30 v/v) of 0.1 M sulfuric acid free of isoproturon after 15 min immersion of the film in a milli Q water solution containing isoproturon at concentrations in the range of 2.5 x 10^{-9} - 5 x 10^{-6} M. The calibration curve is presented in Figure 6A. The square wave voltamogramms clearly showed clearly a current peak increasing with concentration during ISO detection in Figure 6B.

The sensitivity was obtained from the slope of the calibration curve; its value was 4.8701 A/M. The calibration plot was found to be linear between 0 and 10^{-7} M and obeyed the following relation: ***I* (µA) = 4.8701 [Isoproturon] - 0.0043** (R^2=0.9959).

The isoproturon limits of detection (LOD) and quantification (LOQ) that were calculated statistically [78] were 2.76 x 10^{-9} M (0.5 µg L^{-1}) and 9.2 x 10^{-9} M (1.9 µg L^{-1}) respectively.

Repeatability was evaluated after seven analysis replicates of isoproturon 5 x 10^{-7} M solution with a single electrode. Well-shaped voltammograms were obtained for all experiments: the calculated relative standard deviation (RSD) was 7.6 %. Reproducibility of the procedure was evaluated by performing a series of analyses with five different electrodes. The RSD obtained was 12 %. These results indicate that isoproturon MIP-GC electrodes are reliable tools for isoproturon detection and quantification. Each MIP-GC electrode can be used for 25 cycles of analyses with a change of the isoproturon peak intensity less than 20%. Then a decrease of the signal is observed during the 20 next analysis with an extinction of the signal comprising between 50 to 90% depending on the electrode.

3.4.2.2. Interference study

The selectivity of the prepared MIP-GC electrodes toward isoproturon was tested for three interfering molecules (Figure 7): carbendazime, diuron and carbamazepine, at two concentrations, 5 x 10^{-6} M, 5 x 10^{-7} M and 10^{-7} M, for each molecule, in the presence of isoproturon at 5 x 10^{-7} M. These molecules are widely found in environmental waters and have a structure and oxidation potentials quite close to those of isoproturon. Thus, these molecules may interfere with the determination of isoproturon.

The results, presented in Figure 7A and 7B show that according to the RSD found (see previous sub-section), neither carbendazim nor carbamazepine seem to affect the MIP-GC sensitivity toward isoproturon, whereas the presence of diuron (Figure 7C) at the same concentration or at a concentration 10 times higher as isoproturon lowers its signal by 50% and 80% respectively. However, in natural environments, diuron is found at concentrations up to 17 times lower than that of isoproturon [79]. Thus, we can reasonably assume that diuron does not exhibit major interferences with isoproturon.

3.4.2.3. Application of the electrochemical sensors in real water samples

The electrochemical methods developed were applied to the detection of isoproturon in a real water sample. A groundwater sample located in France, Région Centre was chosen in accordance with the funding project (CAPEL MIP, see Acknowledgements). The site is located in the commune of Saint-Rémy-Du-Val (Sarthe, province of Loire-Bretagne region). The monthly monitoring performed in this aquifer revealed that the groundwater is contaminated by several pesticides and notably triazines and chloroacetanilides and their metabolites, but does not contain isoproturon (< 0.005 µg L^{-1}). The samples were prepared with this natural groundwater, adding a known quantity of isoproturon to obtain concentrations from 1 x 10^{-8} to 5 x 10^{-7} M. The calibration plot obtained with these samples was found to be linear between 0 and 5 x 10^{-7} M (shown in Supplementary Material Figure S2) and obeyed the following relation: $\boldsymbol{I}$ **(µA) = 4.1853 [Isoproturon] + 0.0056** (R^2=0.999). The LOD and LOQ were 1.1 x 10^{-8} M (2.2 µg L^{-1}) and 3.7 x 10^{-8} M (7.6 µg L^{-1}), respectively. The sensitivity obtained from the slope of the calibration curve was 4.1853 A/M. The oxidation current of the preconcentrated isoproturon in the MIP film is easily visible in the solutions that contain concentrations higher than 1 x 10^{-8} M of isoproturon.

4 Conclusion

In this work, a novel electrochemical sensor for the sensitive and selective SWV determination of isoproturon, a priority micro-pollutant, was developed. It is shown that ultra-sensitive MIP films for its detection can be prepared in a simple way by CV or CA on GC electrodes. The key parameters of MIP electro-synthesis such as electrodeposition time, scan number, solvent ratio and incubation time were optimized. The extraction step of the template molecule was conducted electrochemically in aqueous solution, thus avoiding the use of toxic organic solvents.

The MIP-GC sensor was able to detect isoproturon in nano-molar concentration with good reproducibility and repeatability. The functionalized electrode surfaces showed good robustness during several analyses.

The performances in terms of LOD, LOQ and selectivity are satisfactory for the contaminated natural waters of the Loire-Bretagne region, where isoproturon concentrations up to 1.2 µg L^{-1} have been measured in 67% of the stations [79]. For other sites, this LOQ is not low enough as worldwide occurrence in the environment showed for effluent a maximum concentration of 0.27 µg/l with a 51% frequency of detection in the effluent of conventional wastewater treatment plants in Europe [78], and for surface water of inland seas a maximum

concentration of 0.06 µg/l with a 100% frequency of detection in estuaries on the Baltic coast [79]. But in spite of these good performances, they are still higher than the maximum allowed levels set by the WFD. Thus, investigations are currently being carried out into the nano-structuration of the polypyrrole path in order to enhance the sensitivity of these sensors and to increase the number of accessible cavities.

Acknowledgements

We gratefully acknowledge the financial support provided to the PIVOTS and the CAPEL-MIP projects by the Region Centre – Val de Loire (ARD 2020 program and CPER 2015 - 2020) and the French Ministry of Higher Education and Research (CPER 2015 -2020 and public service subsidy to CNRS and University of Orleans). This operation is also co-funded by the European Union. Europe is committed to the Center-Val de Loire region with the European Regional Development Fund.

5 References

[1]Nemat Alla MM and Hassan NM, *Pesticide Biochemistry and Physiology*, 2014, **112**, 56–62.

[2]Liang L, Lu YL and Yang H, *Environmental Science and Pollution Research*, 2012, **19**, 2044–2054.

[3] World Health Organization, ed., *Guidelines* for *drinking-water quality,* 2nd ed. Vol.2. Isoproturon in drinking-water,Health criteria and other supporting information. Geneva, 1996.

[4] World Health Organization, ed., *Guidelines for drinking-water quality*, 4th ed, World Health Organization, Geneva, 2011.

[5] Directive 2013/39/UE du parlement européen et du conseil du 12 août 2013 modifiant les directives 2000/60/CE et 2008/105/CE en ce qui concerne les substances prioritaires pour la politique dans le domaine de l'eau, 2013.

[6] Nollet LML and Rathore H.S. eds., Handbook of pesticides: methods of pesticide residues analysis, CRC Press, Boca Raton, Fla., 2010.

[7] Ruberu SR, Draper WM and Perera SK, J. Agric. Food Chem., 2000, **48**, 4109–4115.

[8]Losito I, Amorisco A, Carbonara T, Lofiego S and Palmisano F, *Analytica Chimica Acta,* 2006, **575**, 89–96.

[9]Li Y, George JE, McCarty CL and Wendelken SC, *Journal of Chromatography A*, 2006, **1134**, 170–176.

[10] Hogenboom A, Hofman M, Kok S, Niessen WM and Brinkman UAT, *Journal of Chromatography A*, 2000, **892**, 379–390.

[11] Manisankar P, Vedhi C and Selvanathan G, *Transactions- Society For The Advancement Of Electrochemical Science And Technology*, 2002, **37**, 135–140.

[12] Van der Linden WE and Dieker JW, *Analytica Chimica Acta*, 1980, **119**, 1–24.

[13] Noyrod P, Chailapakul O, Wonsawat W and Chuanuwatanakul S, *Journal of Electroanalytical Chemistry*, 2014, **719**, 54–59.

[14] Manisankar P, Selvanathan G, Viswanathan S and Gurumallesh Prabu H, *Electroanalysis*, 2002, **14**, 1722–1727.

[15] Ivan Svancara, Kurt Kalcher, Alain Walcarius, Karel Vytras, *Electroanalysis with Carbon Paste Electrodes*, CRC Press , 2012.

[16]Vytřas K, Svancara I and Metelka R, *Journal of the Serbian Chemical Society*, 2009, **74**, 1021–1033.

[17] McFadden CF, Melaragno PR and Davis JA, *Analytical Chemistry*, 1990, **62**, 742–746.

[18] Pecková K, Musilová J and Barek J, *Critical Reviews in Analytical Chemistry*, 2009, **39**, 148–172.

[19] Manisankar P, Sundari PA, Sasikumar R and Palaniappan S, *Talanta*, 2008, **76**, 1022–1028.

[20] Su S, Chen S and Fan C, *Green Energy & Environment*, 2017, **3**, 97-106..

[21] Manisankar P, Selvanathan G and Vedhi C, *Applied Clay Science*, 2005, **29**, 249–257.

[22] Manisankar P, Selvanathan G and Vedhi C, *Talanta*, 2006, **68**, 686–692.

[23] Baskeyfield DEH, Davis F, Magan N and Tothill IE, *Analytica Chimica Acta*, 2011, **699**, 223–231.

[24] Haddaoui M and Raouafi N, *Sensors and Actuators B: Chemical*, 2015, **219**, 171–178.

[25] Jiang X, Li D, Xu X, Ying Y, Li Y, Ye Z and Wang J, *Biosensors and Bioelectronics*, 2008, **23**, 1577–1587.

[26] Manisankar P, Selvanathan G and Vedhi C, *International Journal of Environmental Analytical Chemistry*, 2005, **85**, 409–422.

[27] Udomsap D, Branger C, Culioli G, Dollet P and Brisset H, *Chemical Communications*, 2014, **50**, 7488-7491.

[28] Palchetti I., Hansen P., Barcelo D., Past, Present and Future Challenges of Biosensors and Bioanalytical Tools in Analytical Chemistry, 1st Edition, in: *Comprehensive Analytical Chemistry*, vol.77, Elsevier, 2017.

[29]Ramanavičius A, Ramanavičienė A and Malinauskas A, *Electrochimica Acta*, 2006, **51** 6025–6037.

[30] Haupt K and Mosbach K, *Chemical Reviews*, 2000, **100**, 2495–2504.

[31] Maouche N, Guergouri M, Gam-Derouich S, Jouini M, Nessark B and Chehimi M.M, *Journal of Electroanalytical Chemistry*, 2012, **685**, 21–27.

[32] Kotova K, Hussain M, Mustafa G and Lieberzeit PA, *Sensors and Actuators B: Chemical*, 2013, **189**. 199–202.

[33] Chen P-Y, Vittal R, Nien P-C, Liou G-S and Ho K-C, *Talanta*, 2010, **80**, 1145–1151.

[34] Yu J, Wang S, Zhao G, Wang B, Ding L, Zhang X, Xie J and Xie F, *Journal of Chromatography B*, 2014, **958**, 130–135.

[35] Pérez-Moral N and Mayes AG, *Biosensors and Bioelectronics*, 2006, 21, 1798–1803.

[36] Pereira I, Rodrigues MF, Chaves AR and Vaz BG, *Talanta*, 2018, **17**8 , 507–514.

[37] Yao T, Gu X, Li T, Li J, Li J, Zhao Z, Wang J, Qin Y and She Y, *Biosensors and Bioelectronics*, 2016, **75**, 96–100.

[38] Capoferri D, Del Carlo M, Ntshongontshi N, Iwuoha EI, Sergi M, Di Ottavio F and Compagnone D, *Talanta*, 2017, **174**, 599–604.

[39] Iacob B-C, Bodoki E, Farcau C, Barbu-Tudoran L and Oprean R, *Electrochimica Acta*, 2016, **21**7, 195–202.

[40] Zhang YP, Zuo GQ, Gong WJ, Deng YE and Li QM, *Chinese Chemical Letters*, 2007, **18**, 734–737.

[41] Fuchs Y, Soppera O and Haupt K, *Analytica Chimica Acta*, 2012, **717**, 7–20.

[42] Bergmann NM, and Peppas NA, *Progress in Polymer Science*, 2008, 33, 271–288.

[43] Pan G, Zhang Y, Guo X, Li C and Zhang H, *Biosensors and Bioelectronics*, 2010, **2**6 976–982.

[44] Beyazit S, Tse Sum Bui B, Haupt K and Gonzato C, *Progress in Polymer Science*, 2016, **62**, 1–21. doi:10.1016/j.progpolymsci.2016.04.001.

[45] Ton X-A, Acha V, Bonomi P, Tse Sum Bui B and Haupt K, *Biosensors and Bioelectronics*, 2015, **64**, 359–366.

[46] Tiwari A and Uzun L, eds., *Advanced molecularly imprinting materials*, John Wiley & Sons, Inc. ; Scrivener Publishing LLC, Hoboken, New Jersey : Beverly, Massachusetts, 2017.

[47] Wong A, Foguel MV, Khan S, de Oliveira FM, Tarley CRT and Sotomayor MDPT, *Electrochimica Acta*, 2015, **182**, 122–130.

[48] Hrichi H, Monser L and Adhoum N, *Journal of Electroanalytical Chemistry*, 2017, **805**, 133–145.

[49] Florea A, Cristea C, Vocanson F, Săndulescu R and Jaffrezic-Renault N, *Electrochemistry Communications*, 2015, 59, 36–39. .

[50] Luo J, Huang J, Wu Y, Sun J, Wei W and Liu X, *Biosensors and Bioelectronics*, 2017, **94**, 39–46.

[51] Nezhadali A, Mehri L and Shadmehri R, *Materials Science and Engineering: C*, 2018, **85**, 225-232.

[52] Schweiger B, Kim J, Kim Y and Ulbricht M, *Sensors*. 2015, **15**, 4870–4889.

[53] da Silva H, Pacheco JG, Magalhães, JMCS, Viswanathan S and Delerue-Matos C, *Biosensors and Bioelectronics*. 2014, **52**, 56–61.

[54] Maouche N, Guergouri M, Gam-Derouich S, Jouini M, Nessark B and Chehimi MM, *Journal of Electroanalytical Chemistry*. 2012, **685**, 21–27.

[55] Guo Z, Florea A, Jiang M, Mei Y, Zhang W, Zhang A, Săndulescu R and Jaffrezic-Renault N, *Coatings*, 2016, **6**, 42.

[56] Suryanarayanan V, Wu C-T and Ho K-C, *Electroanalysis*, 2010, **22**, 1795–1811.

[57] Maouche N, Guergouri M, Gam-Derouich S, Jouini M, Nessark B and Chehimi MM,

Journal of Electroanalytical Chemistry. 2012, **685**, 21–27.

[58] Khadro B, Sanglar C, Bonhomme A, Errachid A and Jaffrezic-Renault N, *Procedia Engineering*, 2010, **5**, 371–374.

[59] Lu Y, Yan C-L and Gao S-Y, *Applied Surface Science*, 2009, **25**5, 6061–6066.

[60] Su W-X, Rick J and Chou T-C, *Microchemical Journal*. 2009, **92**, 123–128.

[61] Ling T-R, Syu YZ, Tasi Y-C, Chou T-C and Liu C-C, *Biosensors and Bioelectronics*, 2005, **21**, 901–907.

[62] Gam-Derouich S, Jouini M, Ben Hassen-Chehimi D and Chehimi MM, *Electrochimica Acta*, 2012, **73**, 45–52.

[63] Xu Z, Fang G and Wang S, *Food Chemistry*a 2010, **119**, 845–850.

[64] Puoci F, Curcio M, Cirillo G, Iemma F, Spizzirri UG and Picci N, *Food Chemistry*, 2008, **106**, 836–842.

[65] Suedee R, Jantarat C, Lindner W, Viernstein H, Songkro S and Srichana T,

Journal of Controlled Release, 2010, **142**, 122–131.

[66] Akyüz D, Keleş T, Biyiklioglu Z and Koca A, *Journal of Electroanalytical Chemistry*, 2017, **804**, 53–63.

[67] Shahtaheri SJ, Faridbod F and Khadem M, *Procedia Technology*, 2017, **27**, 96–97.

[68] Capoferri D, Del Carlo M, Ntshongontshi N, Iwuoha EI, Sergi M, Di Ottavio F and Compagnone D, *Talanta*, 2017, **174**, 599–604.

[69] Zhao F, She Y, Zhang C, Cao X, Wang S, Zheng L, Jin M, Shao H, Jin F and Wang J,

Journal of Chromatography B, 2017, **1064**, 143–150.

[70] Zhu X, Yang J, Su Q, Cai J and Gao Y, *Journal of Chromatography A*, 2005, **1092**, 161–169.

[71] Li S, Tao H and Li J, *Electroanalysis*, 2012, **24**, 1664–1670.

[72] Singh KP, Prajapati RK, Ahlawat S, Ahlawat S, M. Mungali, S. Kumar, *Open Journal of Applied Biosensor*, 2013, **02**, 20–28.

[73] Fakhry A, Pillier F, Debiemme-Chouvy C, *Journal of Materials Chemistry A*, 2014, **2**, 9859–9865.

[74] Li Y, Conducting Polymers, in: Y. Li (Ed.), *Organic Optoelectronic Materials*, Springer International Publishing, Cham, 2015: pp. 23–50. doi:10.1007/978-3-319-16862-3_2.

[75] Ansari R, *Journal of Chemistry*. 2006, 3, 186–201.

[76] Dejeu J, Taouil AE, Rougeot P, Lakard S, Lallemand F and Lakard B, *Synthetic Metals*, 2010, **160**, 2540–2545.

[77] Downard AJ and Pletcher D, *Journal of Electroanalytical Chemistry and Interfacial Electrochemistry*. 1986, **20**6, 139–145.

[78] Loos R, Carvalho R, António DC, Comero S, Locoro G, Tavazzi S, Paracchini B, Ghiani M, Lettieri T, Blaha L, Jarosova B, Voorspoels S, Servaes K, Haglund P, Fick J, Lindberg RH, Schwesig D and Gawlik , BM, *Water Research*, 2013, **47**, 6475–6487.

[79] Orlikowska A, Fisch K, Schulz-Bull D.E, *Marine Pollution Bulletin*, 2015, **101**, 860–866.

Captions:

Scheme 1: Schematic representation of the procedure used for the preparation of imprinted polypyrrole films on GC substrate MIP GC and the electroanalysis of isoproturon.

Figure 1: Cyclic voltammograms taken during electropolymerization of pyrrole (0.01 M) in absence (NIP) and in presence of ISO (1 mM) (MIP) onto GC electrode, electrolyte: 0.1 M $LiClO_4$ in ethanol/water (20:80 v/v). Scan rate 10 mV s^{-1}.

Figure 2: Influence of the scan number during electropolymerization of the MIP on GC electrode (**A)** on isoproturon response on MIP-GC electrode **(B)** on MIP film thickness estimated using Faraday's law from the voltammogram **(C)** on CV ferrocene response (2.5 mM) in NBu_4BF_4 (0.1 M) acetonitrile solution on bare and MIP-GC electrodes - scan rate 100 $mV.s^{-1}$.

Figure 3: Electropolymerization of MIP-GC electrode for different ratios of ethanol/water with $LiClO_4$ 0.1M (A) film thickness calculated from chronoamperogram and (B) ISO peak intensity electropolymerization : CA 1.1 V during 600 s ; pyrrole 0.01 M in presence of ISO 1 mM.

Figure 4: Effect of electropolymerization time on the electrochemical response of 5 x 10^{-7} M of ISO at the MIP-GC electrode in ethanol/water (70:30 v/v) of H_2SO_4 0.1 M, **(A)** the thickness of the MIP film estimated from the chronoamperogram **(B)** isoproturon electrochemical response, MIP film was formed by chronoamperometry setting the potential at 1.1 V, incubation time 15 min **(C)** comparative study of the MIP film thickness estimated by Faraday's law calculations and by EQCM experiments in order to follow the chronoamperometry electropolymerization process (potential applied 1.1 V, time duration 885 sec) of ISO (1 mM) and pyrrole (0.01 M) on gold quartz used as a working electrode, electrolyte: 0.1 M $LiClO_4$ in ethanol/water (80:20 v/v).

Figure 5: Isoproturon (5 x 10^{-7} M) response on the MIP-GC electrode for different incubation time.

Figure 6: The calibration curves of isoproturon detection obtained at MIP-GC electrode in milli-Q water. Current-concentration calibration curve **(A)** includes linear region for ISO concentration, and calibration linear equation **(B)** square wave voltammograms obtained during electrochemical determination of isoproturon.

Figure 7: Effect of the interferences on the determination of ISO (5 x 10^{-7} M) using the MIP-GC electrode: **(A)** carbamazepine **(B)** carbendazim and **(C)** diuron.

Scheme:

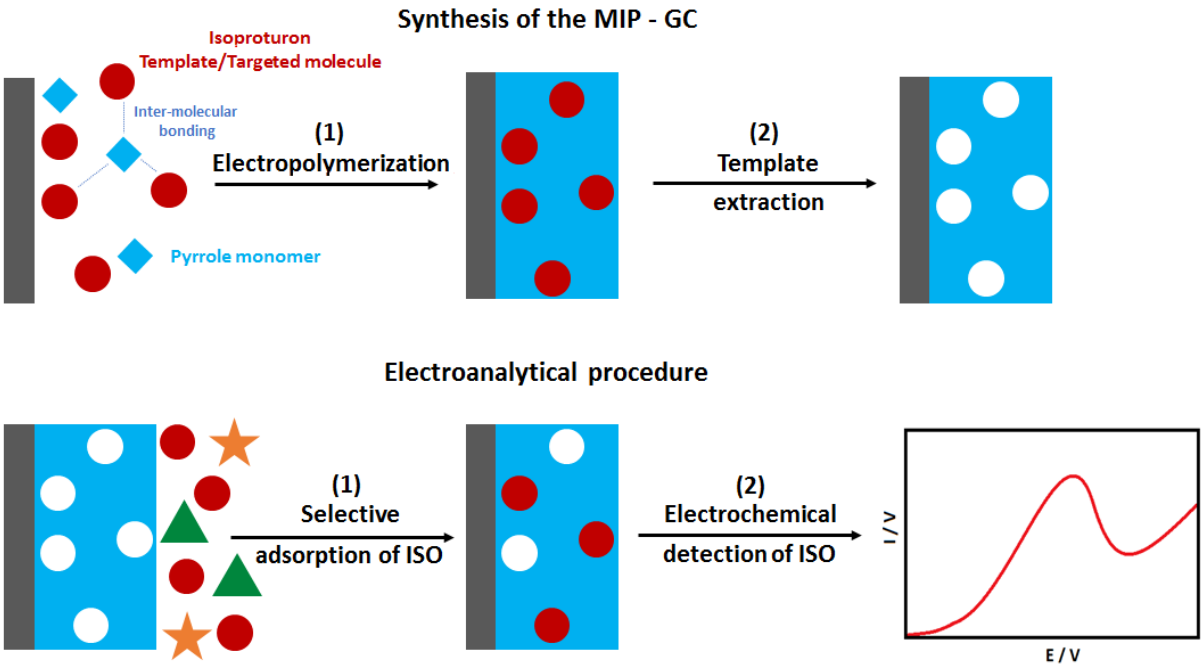

Scheme 1

Figures:

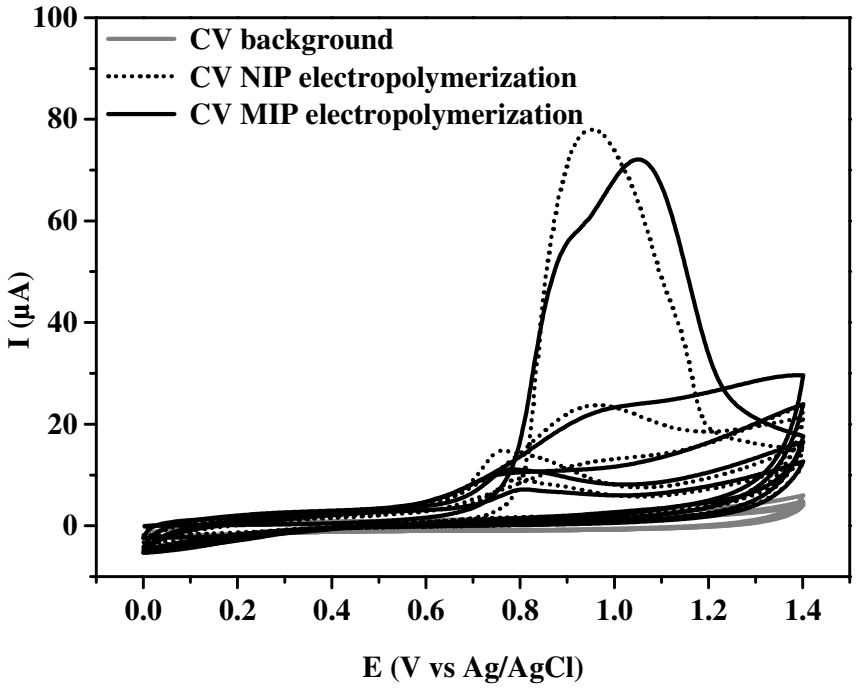

Figure 1

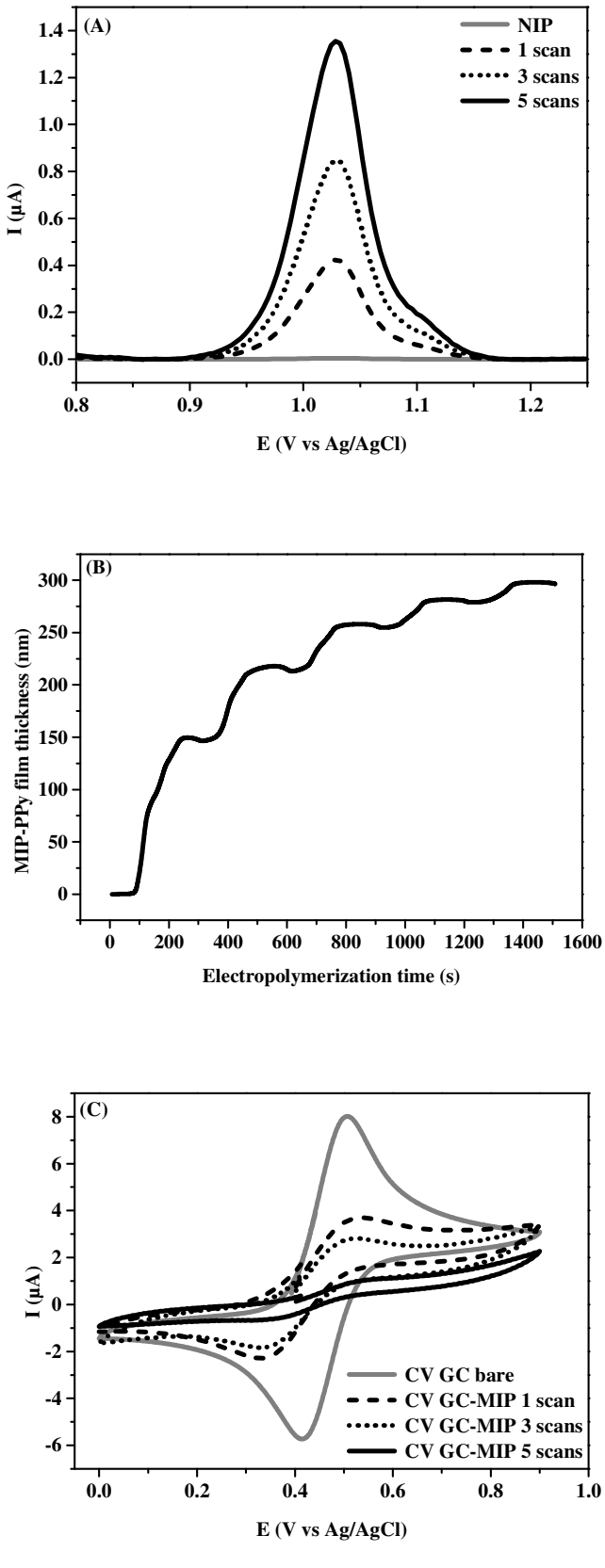
(A)
NIP
1 scan
3 scans
5 scans
I (µA)
E (V vs Ag/AgCl)
(B)
MIP-PPy film thickness (nm)
Electropolymerization time (s)
(C)
CV GC bare
CV GC-MIP 1 scan
CV GC-MIP 3 scans
CV GC-MIP 5 scans
I (µA)
E (V vs Ag/AgCl)

Figure 2

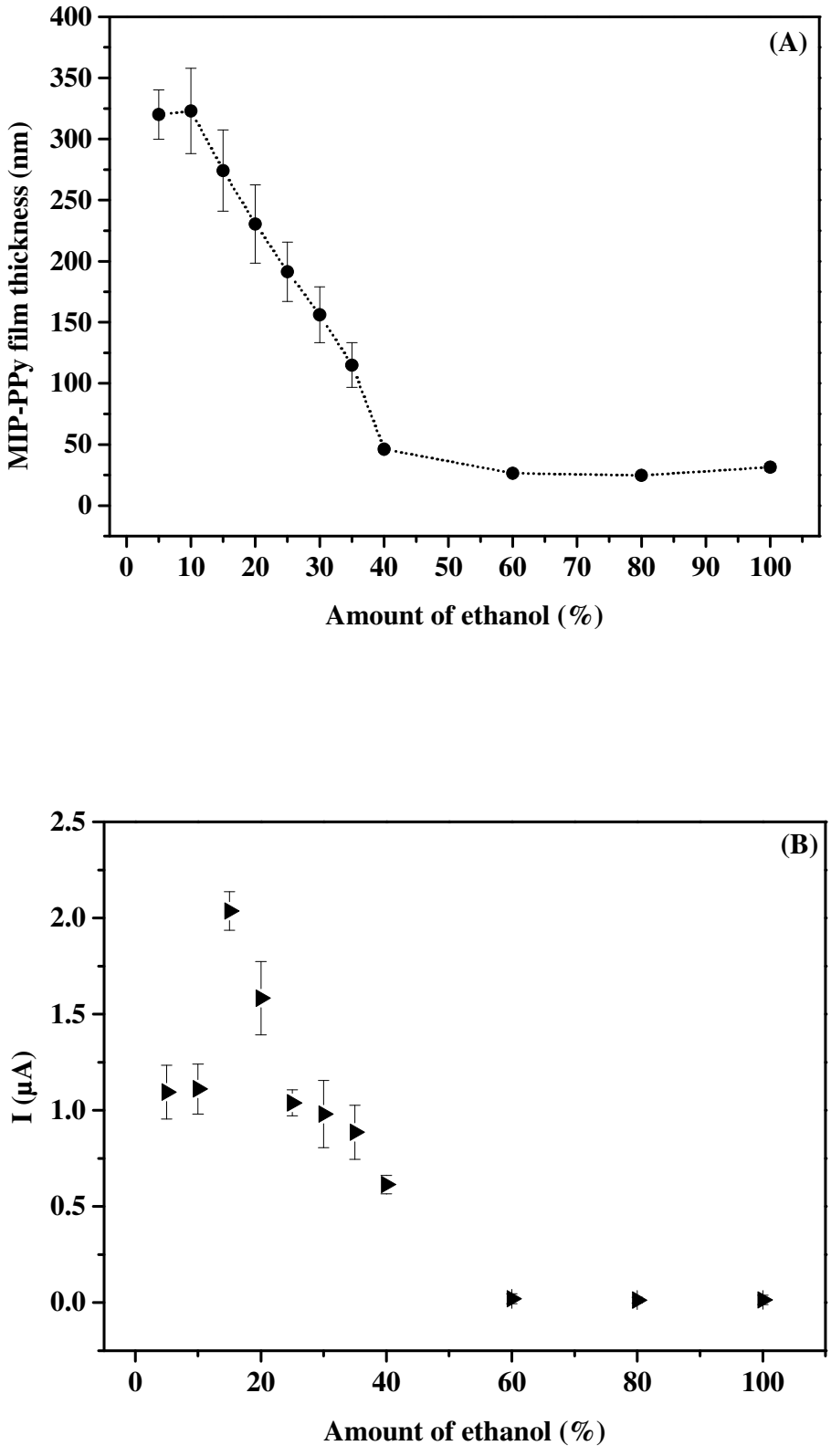
(A)
MIP-PPy film thickness (nm)
400
350
300
250
200
150
100
50
0
0
10
20
30
40
50
60
70
80
90
100
Amount of ethanol (%)
(B)
I (µA)
2.5
2.0
1.5
1.0
0.5
0.0
0
20
40
60
80
100
Amount of ethanol (%)

Figure 3

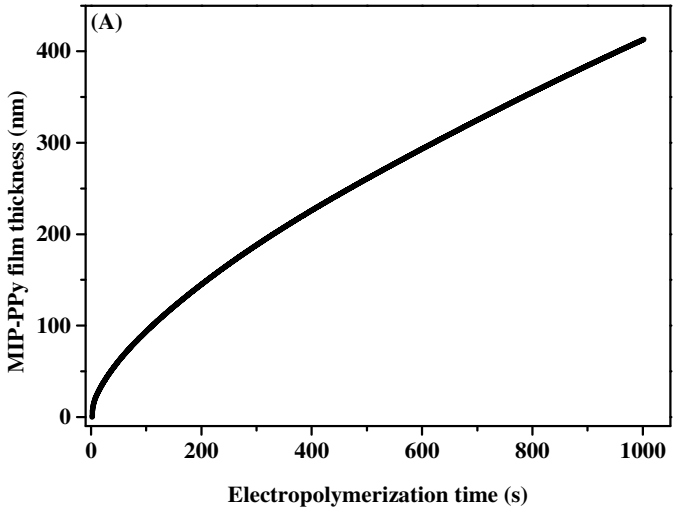
(A)
MIP-PPy film thickness (nm)
0
100
200
300
400
0
200
400
600
800
1000
Electropolymerization time (s)

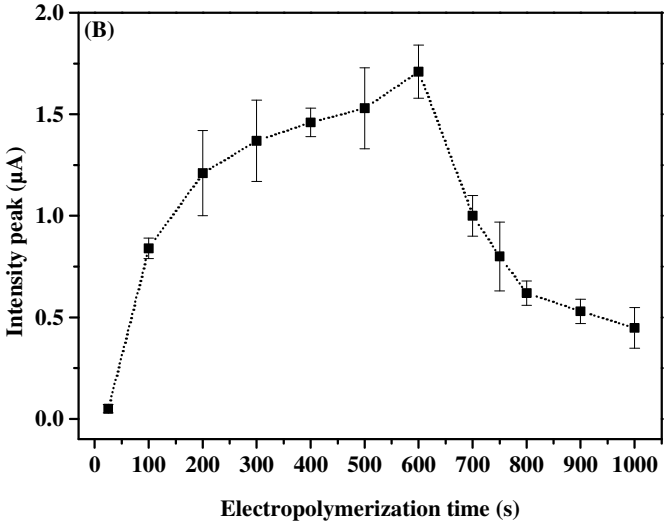
(B)
Intensity peak (µA)
0.0
0.5
1.0
1.5
2.0
0
100
200
300
400
500
600
700
800
900
1000
Electropolymerization time (s)

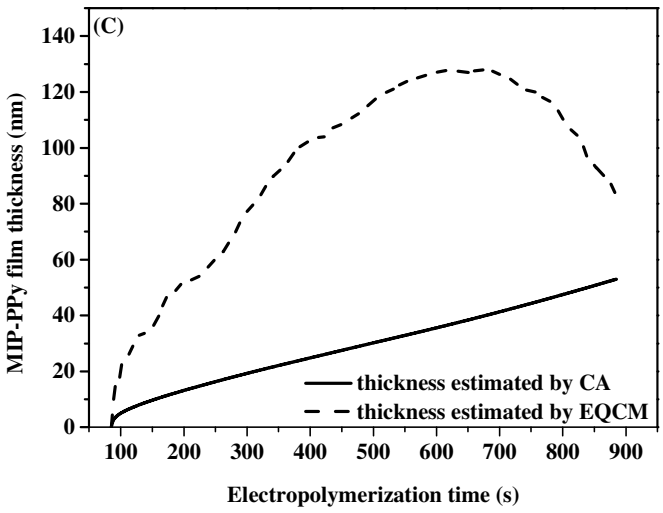
(C)
MIP-PPy film thickness (nm)
0
20
40
60
80
100
120
140
100
200
300
400
500
600
700
800
900
Electropolymerization time (s)
thickness estimated by CA
thickness estimated by EQCM

Figure 4

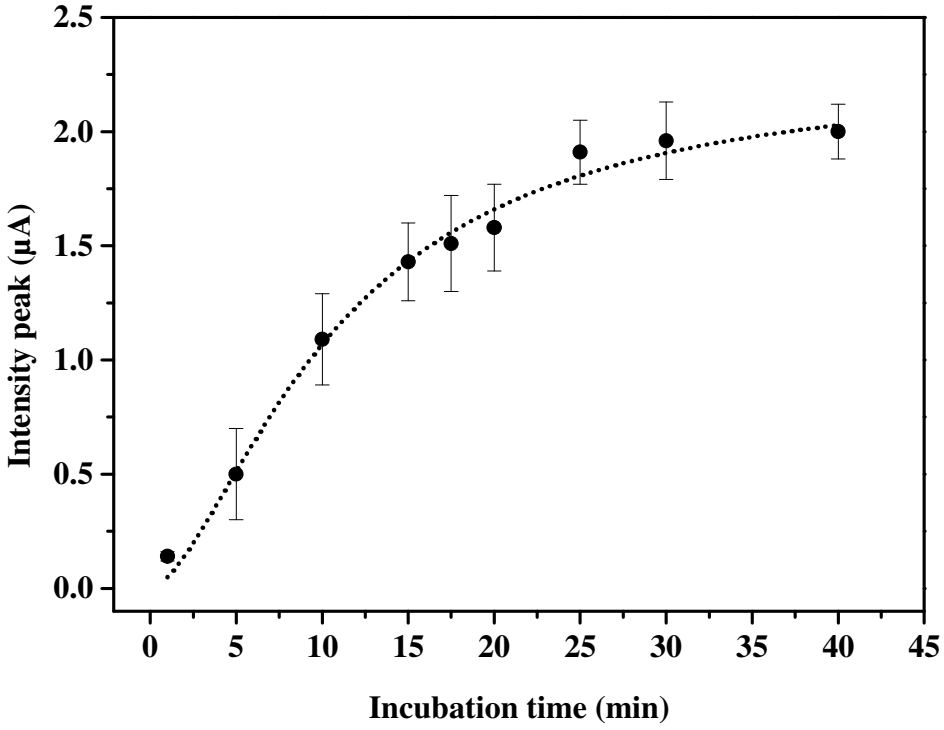

Figure 5

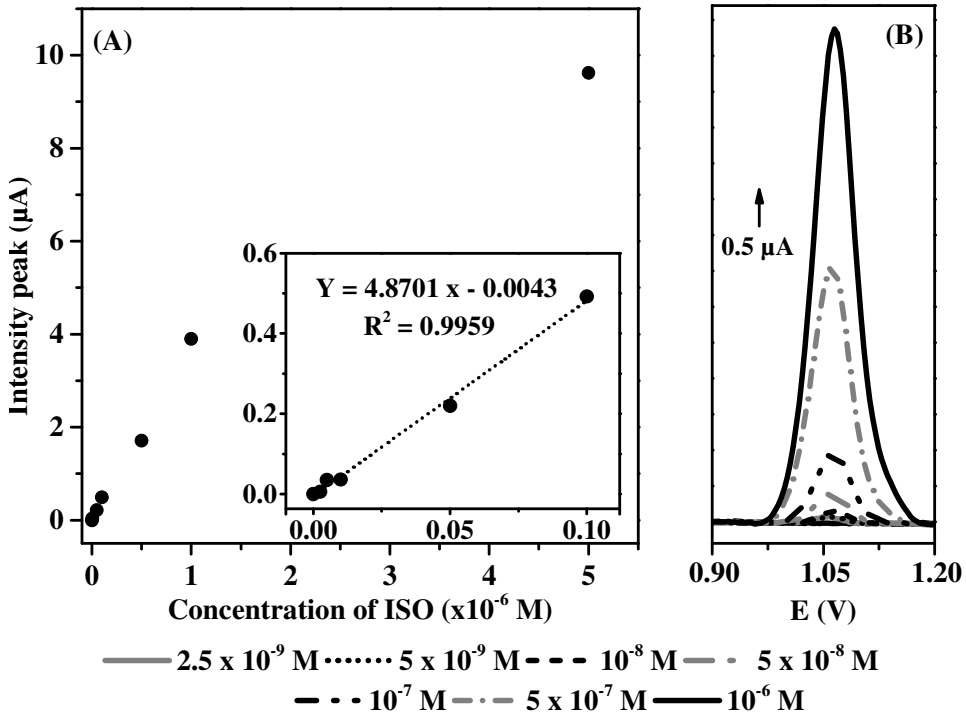

Figure 6

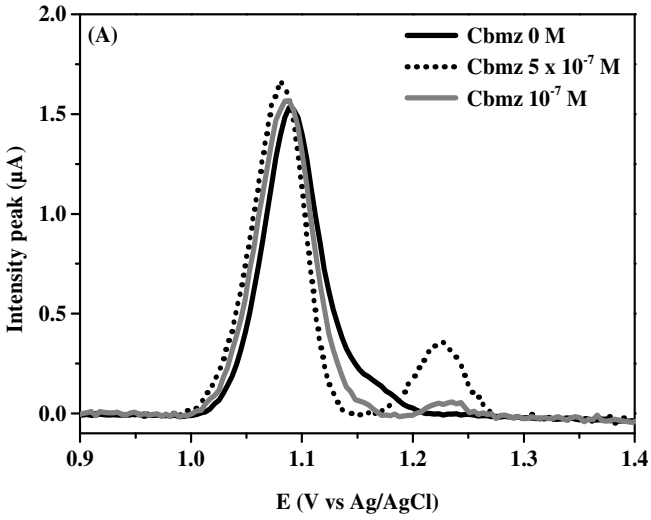
(A)
Cbmz 0 M
Cbmz 5 x 10-7 M
Cbmz 10-7 M
Intensity peak (µA)
E (V vs Ag/AgCl)

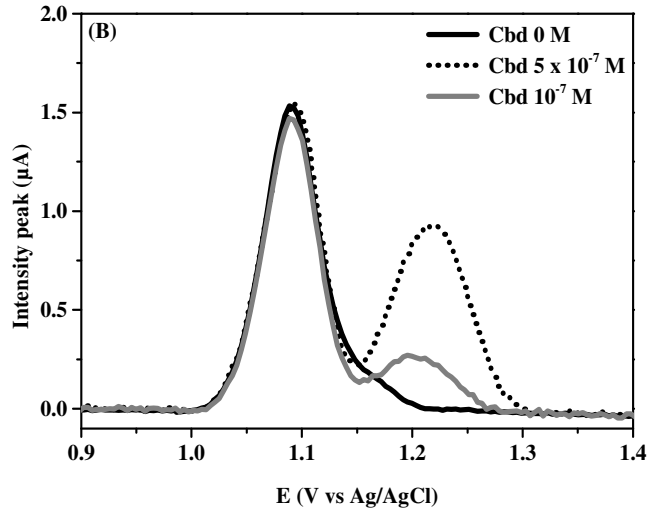
(B)
Cbd 0 M
Cbd 5 x 10-7 M
Cbd 10-7 M
Intensity peak (µA)
E (V vs Ag/AgCl)

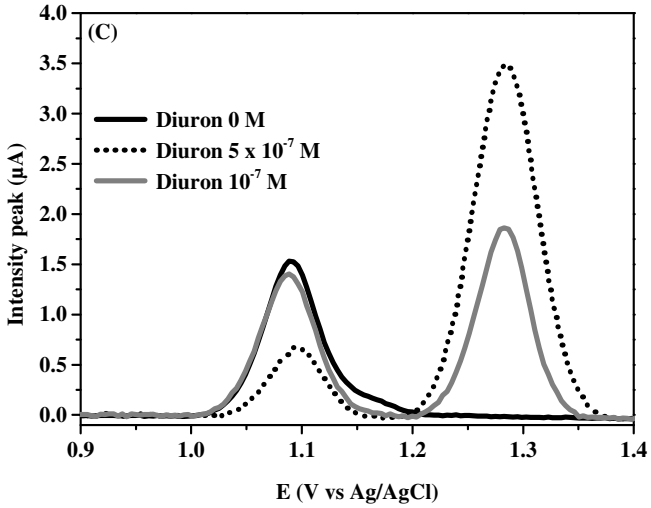
(C)
Diuron 0 M
Diuron 5 x 10-7 M
Diuron 10-7 M
Intensity peak (µA)
E (V vs Ag/AgCl)

Figure 7

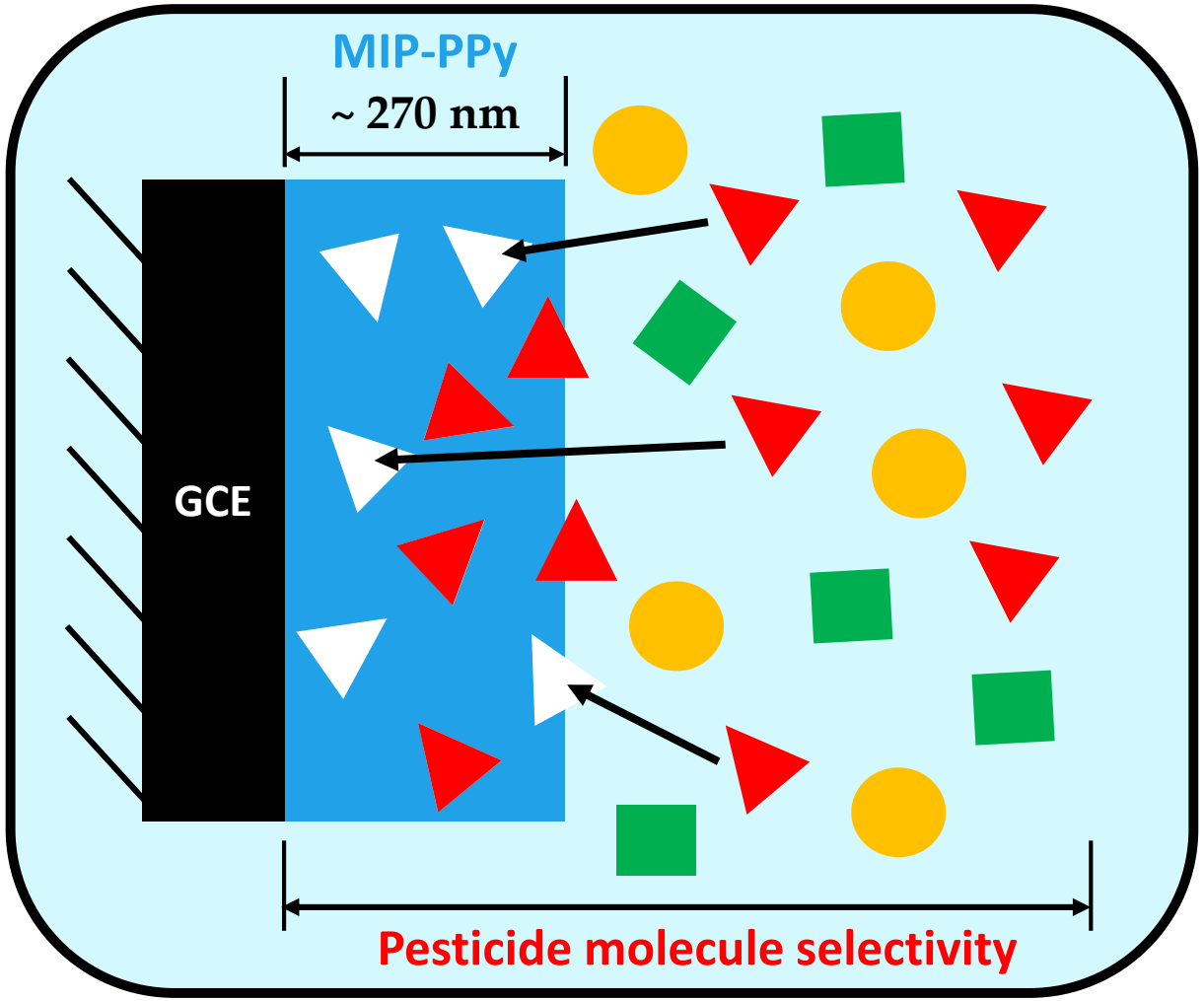
MIP-PPy
~ 270 nm
GCE
Pesticide molecule selectivity

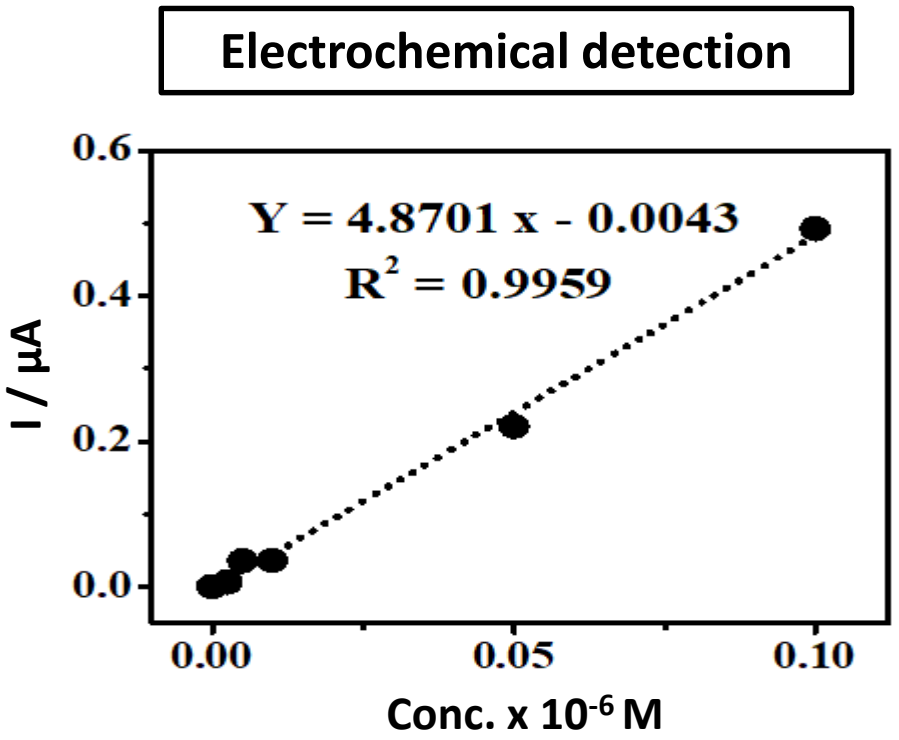
Electrochemical detection
Y = 4.8701 x - 0.0043
R² = 0.9959
I / µA
0.6
0.4
0.2
0.0
0.00
0.05
0.10
Conc. x 10⁻⁶ M